EUROPEAN ORGANISATION FOR NUCLEAR RESEARCH

CERN–PPE/94–91
15 June 1994

Observation of Exclusive Decays of B Mesons at LEP

The OPAL Collaboration

Abstract

Data collected with the OPAL detector at LEP during 1990–1992 are used to study exclusive decays of B mesons. We observe the decay $B^0_d \to D^{*-}\pi^+$ and several B^0_s candidates in the modes $B^0_s \to J/\psi\phi$ and $B^0_s \to D^-_s\pi^+$. Using one unambiguous event in the mode $B^0_s \to J/\psi\phi$, we measure the mass of the B^0_s meson to be $5.359 \pm 0.019 \pm 0.007$ GeV/c^2.

(Submitted to Physics Letters B)

The OPAL Collaboration

R. Akers[16], G. Alexander[23], J. Allison[16], K.J. Anderson[9], S. Arcelli[2], S. Asai[24], A. Astbury[28], D. Axen[29], G. Azuelos[18,a], A.H. Ball[17], R.J. Barlow[16], R. Bartoldus[3], J.R. Batley[5], G. Beaudoin[18], A. Beck[23], G.A. Beck[13], J. Becker[10], C. Beeston[16], T. Behnke[27], K.W. Bell[20], G. Bella[23], P. Bentkowski[18], P. Berlich[10], S. Bethke[32], O. Biebel[32], I.J. Bloodworth[1], P. Bock[11], H.M. Bosch[11], M. Boutemeur[18], P. Bright-Thomas[25], R.M. Brown[20], A. Buijs[8], H.J. Burckhart[8], C. Burgard[27], P. Capiluppi[2], R.K. Carnegie[6], A.A. Carter[13], J.R. Carter[5], C.Y. Chang[17], C. Charlesworth[6], D.G. Charlton[8], S.L. Chu[4], P.E.L. Clarke[15], J.C. Clayton[1], S.G. Clowes[16], I. Cohen[23], J.E. Conboy[15], M. Coupland[14], M. Cuffiani[2], S. Dado[22], C. Dallapiccola[17], G.M. Dallavalle[2], C. Darling[31], S. De Jong[13], H. Deng[17], M. Dittmar[4], M.S. Dixit[7], E. do Couto e Silva[12], J.E. Duboscq[8], E. Duchovni[26], G. Duckeck[8], I.P. Duerdoth[16], U.C. Dunwoody[5], P.A. Elcombe[5], P.G. Estabrooks[6], E. Etzion[23], H.G. Evans[9], F. Fabbri[2], B. Fabbro[21], M. Fanti[2], M. Fierro[2], M. Fincke-Keeler[28], H.M. Fischer[3], R. Folman[26], D.G. Fong[17], M. Foucher[17], H. Fukui[24], A. Fürtjes[8], P. Gagnon[6], A. Gaidot[21], J.W. Gary[4], J. Gascon[18], N.I. Geddes[20], C. Geich-Gimbel[3], S.W. Gensler[9], F.X. Gentit[21], T. Geralis[20], G. Giacomelli[2], P. Giacomelli[4], R. Giacomelli[2], V. Gibson[5], W.R. Gibson[13], J.D. Gillies[20], J. Goldberg[22], D.M. Gingrich[30,a], M.J. Goodrick[5], W. Gorn[4], C. Grandi[2], P. Grannis[8], J. Hagemann[27], G.G. Hanson[12], M. Hansroul[8], C.K. Hargrove[7], J. Hart[8], P.A. Hart[9], P.M. Hattersley[1], M. Hauschild[8], C.M. Hawkes[8], E. Heflin[4], R.J. Hemingway[6], G. Herten[10], R.D. Heuer[8], J.C. Hill[5], S.J. Hillier[8], T. Hilse[10], D.A. Hinshaw[18], P.R. Hobson[25], D. Hochman[26], R.J. Homer[1], A.K. Honma[28,a], R.E. Hughes-Jones[16], R. Humbert[10], P. Igo-Kemenes[11], H. Ihssen[11], D.C. Imrie[25], A. Jawahery[17], P.W. Jeffreys[20], H. Jeremie[18], M. Jimack[1], M. Jones[6], R.W.L. Jones[8], P. Jovanovic[1], C. Jui[4], D. Karlen[6], K. Kawagoe[24], T. Kawamoto[24], R.K. Keeler[28], R.G. Kellogg[17], B.W. Kennedy[15], J. King[13], S. Kluth[5], T. Kobayashi[24], M. Kobel[10], D.S. Koetke[8], T.P. Kokott[3], S. Komamiya[24], R. Kowalewski[8], R. Howard[29], J. von Krogh[11], P. Kyberd[13], G.D. Lafferty[16], H. Lafoux[8], R. Lahmann[17], J. Lauber[8], J.G. Layter[4], P. Leblanc[18], P. Le Du[21], A.M. Lee[31], E. Lefebvre[18], M.H. Lehto[15], D. Lellouch[26], C. Leroy[18], J. Letts[4], L. Levinson[26], Z. Li[12], S.L. Lloyd[13], F.K. Loebinger[16], G.D. Long[17], B. Lorazo[18], M.J. Losty[7], X.C. Lou[8], J. Ludwig[10], A. Luig[10], M. Mannelli[8], S. Marcellini[2], C. Markus[3], A.J. Martin[13], J.P. Martin[18], T. Mashimo[24], P. Mättig[3], U. Maur[3], J. McKenna[29], T.J. McMahon[1], A.I. McNab[13], J.R. McNutt[25], F. Meijers[8], F.S. Merritt[9], H. Mes[7], A. Michelini[8], R.P. Middleton[20], G. Mikenberg[26], J. Mildenberger[6], D.J. Miller[15], R. Mir[12], W. Mohr[10], C. Moisan[18], A. Montanari[2], T. Mori[24], M. Morii[24], U. Müller[3], B. Nellen[3], B. Nijjhar[16], S.W. O'Neale[1], F.G. Oakham[7], F. Odorici[2], H.O. Ogren[12], C.J. Oram[28,a], M.J. Oreglia[9], S. Orito[24], J.P. Pansart[21], P. Paschievici[26], G.N. Patrick[20], M.J. Pearce[1], P. Pfister[10], P.D. Phillips[16], J.E. Pilcher[9], J. Pinfold[30], D. Pitman[28], D.E. Plane[8], P. Poffenberger[28], B. Poli[2], A. Posthaus[3], T.W. Pritchard[13], H. Przysiezniak[18], M.W. Redmond[8], D.L. Rees[8], M. Rison[5], S.A. Robins[13], D. Robinson[5], J.M. Roney[28], E. Ros[8], S. Rossberg[10], A.M. Rossi[2], M. Rosvick[28], P. Routenburg[30], K. Runge[10], O. Runolfsson[8], D.R. Rust[12], M. Sasaki[24], C. Sbarra[2], A.D. Schaile[26], O. Schaile[10], F. Scharf[3], P. Scharff-Hansen[8], P. Schenk[4], B. Schmitt[3], H. von der Schmitt[11], M. Schröder[12], H.C. Schultz-Coulon[10], P. Schütz[3], M. Schulz[8], C. Schwick[27], J. Schwiening[3], W.G. Scott[20], M. Settles[12], T.G. Shears[5], B.C. Shen[4], C.H. Shepherd-Themistocleous[7], P. Sherwood[15], G.P. Siroli[2], A. Skillman[16], A. Skuja[17], A.M. Smith[8], T.J. Smith[28], G.A. Snow[17], R. Sobie[28], R.W. Springer[17], M. Sproston[20], A. Stahl[3], C. Stegmann[10], K. Stephens[16], J. Steuerer[28], R. Ströhmer[11], D. Strom[19], H. Takeda[24], S. Tarem[8], M. Tecchio[9], P. Teixeira-Dias[11], N. Tesch[3], M.A. Thomson[15], S. Towers[6], T. Tsukamoto[24], M.F. Turner-Watson[8], D. Van den plas[18], R. Van Kooten[12], G. Vasseur[21], M. Vincter[28], A. Wagner[27], D.L. Wagner[9], C. Wahl[10], C.P. Ward[5], D.R. Ward[5], J.J. Ward[15], P.M. Watkins[1], A.T. Watson[1], N.K. Watson[7], P. Weber[6], P.S. Wells[8], N. Wermes[3], B. Wilkens[10], G.W. Wilson[4], J.A. Wilson[1], V-H. Winterer[10], T. Wlodek[26], G. Wolf[26], S. Wotton[11], T.R. Wyatt[16], R. Yaari[26], A. Yeaman[13], G. Yekutieli[26], M. Yurko[18], W. Zeuner[8], G.T. Zorn[17].

[1]School of Physics and Space Research, University of Birmingham, Birmingham B15 2TT, UK
[2]Dipartimento di Fisica dell' Università di Bologna and INFN, I-40126 Bologna, Italy
[3]Physikalisches Institut, Universität Bonn, D-53115 Bonn, Germany
[4]Department of Physics, University of California, Riverside CA 92521, USA
[5]Cavendish Laboratory, Cambridge CB3 0HE, UK
[6]Carleton University, Department of Physics, Colonel By Drive, Ottawa, Ontario K1S 5B6, Canada
[7]Centre for Research in Particle Physics, Carleton University, Ottawa, Ontario K1S 5B6, Canada
[8]CERN, European Organisation for Particle Physics, CH-1211 Geneva 23, Switzerland
[9]Enrico Fermi Institute and Department of Physics, University of Chicago, Chicago IL 60637, USA
[10]Fakultät für Physik, Albert Ludwigs Universität, D-79104 Freiburg, Germany
[11]Physikalisches Institut, Universität Heidelberg, D-69120 Heidelberg, Germany
[12]Indiana University, Department of Physics, Swain Hall West 117, Bloomington IN 47405, USA
[13]Queen Mary and Westfield College, University of London, London E1 4NS, UK
[14]Birkbeck College, London WC1E 7HV, UK
[15]University College London, London WC1E 6BT, UK
[16]Department of Physics, Schuster Laboratory, The University, Manchester M13 9PL, UK
[17]Department of Physics, University of Maryland, College Park, MD 20742, USA
[18]Laboratoire de Physique Nucléaire, Université de Montréal, Montréal, Quebec H3C 3J7, Canada
[19]University of Oregon, Department of Physics, Eugene OR 97403, USA
[20]Rutherford Appleton Laboratory, Chilton, Didcot, Oxfordshire OX11 0QX, UK
[21]CEA, DAPNIA/SPP, CE-Saclay, F-91191 Gif-sur-Yvette, France
[22]Department of Physics, Technion-Israel Institute of Technology, Haifa 32000, Israel
[23]Department of Physics and Astronomy, Tel Aviv University, Tel Aviv 69978, Israel
[24]International Centre for Elementary Particle Physics and Department of Physics, University of Tokyo, Tokyo 113, and Kobe University, Kobe 657, Japan
[25]Brunel University, Uxbridge, Middlesex UB8 3PH, UK
[26]Particle Physics Department, Weizmann Institute of Science, Rehovot 76100, Israel
[27]Universität Hamburg/DESY, II Institut für Experimental Physik, Notkestrasse 85, D-22607 Hamburg, Germany
[28]University of Victoria, Department of Physics, P O Box 3055, Victoria BC V8W 3P6, Canada
[29]University of British Columbia, Department of Physics, Vancouver BC V6T 1Z1, Canada
[30]University of Alberta, Department of Physics, Edmonton AB T6G 2J1, Canada
[31]Duke University, Dept of Physics, Durham, NC 27708-0305, USA
[32]Technische Hochschule Aachen, III Physikalisches Institut, Sommerfeldstrasse 26-28, D-52056 Aachen, Germany

[a]Also at TRIUMF, Vancouver, Canada V6T 2A3

1 Introduction

One of the main goals of b quark studies at LEP is the determination of the masses and lifetimes of b-flavoured hadrons. The masses of the B_u^+ and B_d^0 mesons[1] have been measured by the CLEO and ARGUS experiments from data collected at the $\Upsilon(4S)$ resonance [1]. At LEP, semileptonic decays of b-flavoured hadrons have been studied to establish evidence for the B_s^0 meson and the Λ_b baryon and to determine their lifetimes [2]. In a previous publication [3], based on data collected during 1990–1991, we reported the first observation of one fully reconstructed B_s^0 decay candidate in the mode $B_s^0 \to J/\psi\phi$. Recently, the ALEPH, DELPHI and CDF collaborations [4] have also reported the observation of such events and determined the mass of the B_s^0 meson. In this work we describe a search for exclusive decays of B_d^0 and B_s^0 mesons into several hadronic final states using data collected with the OPAL detector at LEP during the 1990-1992 runs.

The dominant B meson decays are $B \to D(n\pi)$, where D denotes a charmed meson. In addition, a small fraction of the decays contain a J/ψ meson in the final state. The difficulty in reconstructing exclusive hadronic B decays is due to their small branching ratios [5] [6] and the large particle multiplicities involved that result in large combinatorial backgrounds. In this work we limit the analysis to decay modes where both the B and the cascade charmed mesons D^{*-}, D_s^- and J/ψ decay into low-multiplicity final states. We present results on the exclusive decay $B_d^0 \to D^{*-}\pi^+$ and candidate events for the decays $B_s^0 \to D_s^-\pi^+$ and $B_s^0 \to J/\psi\phi$.

2 The OPAL Detector and the Data Sample

The OPAL detector is discussed in detail elsewhere [7]. Here we briefly describe the components which are relevant to this analysis. Charged particle tracking is performed by the central detector system which is located in an axial magnetic field of 0.435 T. The central tracking system consists of a two layer silicon microvertex detector [8], a high precision vertex drift chamber, a large volume jet chamber and a set of z chambers measuring track coordinates along the beam direction. The momentum resolution of the central detector in the plane perpendicular to the beam direction is $(\delta p_{xy}/p_{xy})^2 = (2\%)^2 + (0.15\% \cdot p_{xy})^2$, where p_{xy} is in GeV/c [9]. Particle identification is provided by the measurement of specific ionisation, dE/dx, in the jet chamber. The dE/dx resolution for tracks with the maximum 159 samplings in the jet chamber is 3.5% [10]. The central detector is surrounded by a lead glass electromagnetic calorimeter with a pre-sampler. The magnet yoke is instrumented with layers of streamer tubes which serve as a hadron calorimeter, and provide additional information for muon identification. Four layers of planar drift chambers surrounding the detector provide the tracking for muons.

Data collected by the OPAL detector during 1990–1992 are used in this study corresponding to a total of 1.23×10^6 hadronic Z^0 decays. The selection of hadronic events, with an efficiency of $(98.4 \pm 0.4)\%$, is described elsewhere [11].

For this analysis we impose the following additional requirements on charged tracks: the number of hits in the central detector used for the reconstruction of a track must be greater than 40 (this restricts the acceptance to $|\cos\theta| < 0.94$); the distance of closest approach to the beam axis in the $x-y$ plane must be less than 0.5 cm; the distance to the interaction point along the beam axis at the point of closest approach in the $x-y$ plane must be less than 40 cm; and the transverse momentum with respect to the beam direction must exceed 0.25 GeV/c.

[1] Charge conjugate states are implied throughout this paper.

A track is identified as a pion if the probability of the measured $\mathrm{d}E/\mathrm{d}x$ to be due to a pion is greater than 1%. Tracks are identified as kaons if the $\mathrm{d}E/\mathrm{d}x$ probability for the kaon hypothesis is greater than 5%.

The electron and muon identification criteria are described in detail in a recent publication [12]. In brief, electrons are identified using the measurements of their momentum and $\mathrm{d}E/\mathrm{d}x$ in the central detector and their energy in the electromagnetic calorimeter and the pre-sampler. Muons are identified using a geometrical matching between tracks reconstructed in the central tracking system and track segments.

We use a Monte Carlo simulation to determine the reconstruction and selection efficiencies for the relevant B decays and for the various processes contributing to the background. The JETSET 7.2 parton shower Monte Carlo generator [13] with full simulation of the OPAL detector [14] is used to simulate the decay $\mathrm{Z}^0 \to \mathrm{b\bar{b}}$. For the fragmentation of heavy quarks we use the Peterson fragmentation function [15] with parameters tuned to OPAL data [16]. Data and Monte Carlo simulated events are passed through the same reconstruction programs.

3 Search for Exclusive B^0_d and B^0_s Decays

Exclusive B^0_d and B^0_s decays must be distinguished from a large background from the production of light quark flavours as well as combinatorial background from tracks in $\mathrm{b\bar{b}}$ events. Due to the small branching ratios of exclusive channels and the expected small number of reconstructed events, it is essential to require tight selection criteria that reduce the background to a negligible level.

The analyses proceed by the following steps:
a) Jets of particles in the events are constructed using charged tracks and neutral clusters that are not associated to any charged track. To form jets we use the scaled invariant mass jet-finding algorithm of JADE [17] with a jet resolution parameter $y_\mathrm{cut} = 0.04$.
b) Charmed mesons are reconstructed by forming combinations of charged tracks identified as pions or kaons separately for each jet. This serves to suppress background from light flavour production.
c) Charmed meson candidates are combined with other tracks in the same jet to form B meson candidates. To reduce the contamination of background processes with leptons in the final states we reject charged tracks that are identified as an electron and a muon.
In the following we describe the analysis of each decay mode separately.

3.1 The Decay $\mathrm{B}^0_\mathrm{d} \to \mathrm{D}^{*-}\pi^+$

D^{*-} candidates are identified in the mode $\mathrm{D}^{*-} \to \bar{\mathrm{D}}^0\pi^-$ followed by $\bar{\mathrm{D}}^0 \to \mathrm{K}^+\pi^-$. We form track combinations of $\mathrm{K}^+\pi^-\pi^-$. The invariant mass of a $\mathrm{K}^+\pi^-$ pair is required to be between 1.77 and 1.95 $\mathrm{GeV/c^2}$, consistent with the $\bar{\mathrm{D}}^0$ mass of 1.8645 $\mathrm{GeV/c^2}$. The invariant mass difference $M(\mathrm{K}^+\pi^-\pi^-) - M(\mathrm{K}^+\pi^-)$ is required to be within ± 0.005 $\mathrm{GeV/c^2}$ of the known D^{*-} and $\bar{\mathrm{D}}^0$ mass difference of 0.1454 $\mathrm{GeV/c^2}$ [5]. Candidates for the decay $\mathrm{B}^0_\mathrm{d} \to \mathrm{D}^{*-}\pi^+$ are formed by combining the D^{*-} candidates with each of the remaining positively charged tracks in the same jet.

Characteristic angular distributions of the decay $\mathrm{B}^0_\mathrm{d} \to \mathrm{D}^{*-}\pi^+$ are used to reduce the combinatorial background. Since the B^0_d meson is a pseudoscalar, its decay products are isotropically distributed in its rest frame, in contrast to the combinatorial background which is observed to peak in the forward

or backward directions. We thus require $|\cos\theta_b| < 0.8$, where θ_b is the angle in the B^0_d rest frame between the D^{*-} direction and the direction of the B^0_d in the laboratory frame. The same argument holds for the decay products of the $\bar{D}^0$ meson. We thus require $|\cos\theta_d| < 0.8$, where θ_d is the angle in the $\bar{D}^0$ rest frame between the K^+ direction and the direction of the $\bar{D}^0$ in the laboratory frame.

Angular momentum conservation requires that the spin vector of D^{*-} be in a plane perpendicular to its direction of motion in the B^0_d rest frame. In the rest frame of the D^{*-}, this gives rise to a $\cos^2\theta_v$ distribution, where θ_v is the angle between the $\bar{D}^0$ direction and the D^{*-} direction in the rest frame of the B^0_d. The combinatorial background is observed to be uniformly distributed. We thus require $|\cos\theta_v| > 0.4$.

The long lifetime of B^0_d mesons allows us to suppress further the combinatorial background. For each B^0_d candidate we determine the $\bar{D}^0$ decay vertex and the B^0_d decay vertex (the latter is determined from the intersection of the $\bar{D}^0$ momentum vector with other tracks in the B^0_d decay). We require both decay vertices to be in the hemisphere centred around the B^0_d momentum vector. The efficiency of this requirement is 84%.

Finally, we take advantage of the hard fragmentation of the b quark by requiring the reconstructed momentum of the B^0_d candidate to exceed 70% of the beam energy. This rejects approximately 70% of the remaining combinatorial background, while retaining 65% of the signal.

After all selection criteria, eleven B^0_d candidates remain in the data sample, in the mass range of 4.5 to 6.0 GeV/c^2. The invariant mass distribution of the B^0_d candidates (Fig. 1) shows an enhancement near the B^0_d meson mass of 5.2787 GeV/c^2 [5]. To check the level of the remaining combinatorial background, we examine the invariant mass distribution of the wrong-sign combinations, $D^{*-}\pi^-$. No such event survives our selection in the above mass range.

Possible sources of $D^{*-}\pi^+$ candidates are (a) the signal, $B^0_d \to D^{*-}\pi^+$, (b) random combinatorial background, and (c) feed-down from higher multiplicity decay modes of the B^0_d mesons. Feed-down refers to partially reconstructed decays where one or more particles from the original decay process are undetected or are not included in the reconstruction. The solid histogram in Fig. 2 shows the invariant mass distribution of $D^{*-}\pi^+$ combinations from a sample of simulated events of the type: $Z^0 \to b\bar{b}$ followed by $\bar{b} \to B^0_d$ and $B^0_d \to D^{*-}\pi^+$. From this sample we determine the efficiency for the reconstruction of the decay $B^0_d \to D^{*-}\pi^+$ to be (18 ± 1)% and the mass resolution to be 0.060 GeV/c^2. The quoted uncertainty in the detection efficiency is predominantly statistical. The systematic uncertainties are negligible compared to the statistical error and are ignored.

We search for feed-down effects from several other B^0_d decay modes including the semileptonic decay[2] $B^0_d \to D^{*-}\ell^+\nu$ and higher multiplicity hadronic decays. Due to the dE/dx selection criteria and the rejection of tracks identified as leptons, we find negligible contribution from the semileptonic events. We estimate less than 1.5 events at 90% confidence level (C.L.) in the mass range 4.5 to 6.0 GeV/c^2. However, the decay $B^0_d \to D^{*-}\rho^+$, where $\rho^+ \to \pi^+\pi^0$, produces a broad structure in the $D^{*-}\pi^+$ mass distribution near the B^0_d mass, which is shown by the dashed histogram in Fig. 2. The normalisation is done according to the known relative branching ratios [5]. This results in a distortion of the shape of the expected signal in the $B^0_d \to D^{*-}\pi^+$ mass distribution.

The invariant mass distribution of Fig. 1 is fitted, using a maximum likelihood fit, to two Gaussian distributions representing the decays $B^0_d \to D^{*-}\pi^+$ and $B^0_d \to D^{*-}\rho^+$ (with the Monte Carlo predicted r.m.s widths of 0.060 GeV/c^2 and 0.150 GeV/c^2, respectively), plus a flat distribution for the combinatorial background. The mean of the function representing the $D^{*-}\rho^+$ effect is fixed to

[2]The semileptonic events can contribute to the $D^{*-}\pi^+$ combinations if the lepton is misidentified as a pion.

the prediction from simulation studies. The fit yields 8.1 ± 2.9 $B_d^0 \to D^{*-}\pi^+$ events at an invariant mass of 5.279 ± 0.023 GeV/c^2, and 2.9 ± 1.9 $B_d^0 \to D^{*-}\rho^+$ events. The errors are statistical only as determined by the fit. We repeated the analysis using different sets of cuts. The observed numbers of candidates were within expectations. In addition, we investigated possible systematic uncertainties due to the fitting procedure, we performed a similar fit to the Monte Carlo sample. The fit yielded results consistent with the input values. We conclude that systematic errors from this source are small compared to the statistical uncertainties.

We estimate the branching ratio $B(B_d^0 \to D^{*-}\pi^+)$ from:

$$B = \frac{N(B_d^0)}{2 \cdot N(Z^0) \cdot \Gamma_{b\bar{b}}/\Gamma_{had} \cdot f(\bar{b} \to B_d^0) \cdot B(D^{*-} \to \bar{D}^0\pi^-) \cdot B(\bar{D}^0 \to K^+\pi^-) \cdot \epsilon} \ ,$$

where $N(Z^0)$ is the number of hadronic Z^0 events and ϵ is the detection efficiency for the $K^+\pi^-\pi^-\pi^+$ final state. The Standard Model value for $\Gamma_{b\bar{b}}/\Gamma_{had} = 0.217$ [18], and the B_d^0 production fraction $f(\bar{b} \to B_d^0) = 0.38$ [19] are used. No theoretical errors have been assigned to $\Gamma_{b\bar{b}}/\Gamma_{had}$ and $f(\bar{b} \to B_d^0)$. We find

$$B(B_d^0 \to D^{*-}\pi^+) = (1.0 \pm 0.4 \pm 0.1)\% \ ,$$

where the first error is statistical and the second accounts for uncertainties in the branching ratios of the $\bar{D}^0$ and D^{*-} decays. The systematic error due to uncertainties in the reconstruction efficiency is significantly smaller than the above, and is not included. This measurement is consistent with the Particle Data Group value of $0.33 \pm 0.12\%$ [5].

3.2 The Decay $B_s^0 \to J/\psi\phi$

A unique feature of this decay mode is that it is free from feed-down effects which are present in other decay modes such as $B_s^0 \to D_s^-\pi^+$ decays. Hence its observation allows for a more reliable and direct measurement of the mass of the B_s^0 meson.

Previously, we reported the observation of one $B_s^0 \to J/\psi\phi$ event based on data collected during 1990–1991, with a mass of 5.360 ± 0.070 GeV/c^2 [3]. For this process, we identify the J/ψ meson candidates using the leptonic decay modes $J/\psi \to e^+e^-$ and $J/\psi \to \mu^+\mu^-$. The reported event contained a $J/\psi \to e^+e^-$ candidate. The ϕ meson candidates are identified in the mode $\phi \to K^+K^-$. A possible background to this process is from the decay mode $B_d^0 \to J/\psi K^+\pi^-$, where the pion is mis-identified as a kaon. We find, however, that the invariant mass of the track combinations forming the B_s^0 candidate is inconsistent with the B_d^0 mass if the pion mass is assigned to either of the kaon candidates. Further details on the requirements for the selection and reconstruction of this mode can be found in [3]. No more $B_s^0 \to J/\psi\phi$ events have been found in the data recorded during 1992.

The error assigned to the measured mass of the B_s^0 candidate in [3] was that for a typical reconstructed $J/\psi\phi$ event, as obtained from determining the mass resolution of an ensemble of simulated signal events. This event is shown in Fig. 3. We have reanalyzed this event taking into account the measurement errors of the track parameters of each track used in the reconstruction of the B_s^0 candidate. The e^+ and e^- tracks have been kinematically fitted to the J/ψ hypothesis, and the K^+ and K^- tracks have been kinematically fitted to the ϕ hypothesis. For the B_s^0 candidate an invariant mass of 5.359 ± 0.019 GeV/c^2 is obtained. The indicated uncertainty is due to the errors in track parameters and their covariances after the kinematic refit.

To estimate the systematic error of this mass measurement we performed several checks. In order to check the mass scale, we studied a sample of D^{*-} decays in the mode $D^{*-} \to \bar{D}^0\pi^-$. The difference

in the central value of the D^0 mass from the PDG value, scaled by the B to D meson mass ratio, gives an estimated error of 0.005 GeV/c^2 on the absolute mass scale. The track covariances do not always contain all contributions from systematic errors of the momentum measurement. Allowing additional systematic contributions to the measured covariances (due to unmodeled alignment errors, wire bowing and multiple scattering) leads to an additional estimated systematic error of 0.004 GeV/c^2. Adding these two contributions in quadrature gives a total estimated systematic error of 0.007 GeV/c^2, resulting in a B_s^0 invariant mass of $5.359 \pm 0.019 \pm 0.007$ GeV/c^2.

The efficiencies to detect the $J/\psi \to \mu^+\mu^-$ and $J/\psi \to e^+e^-$ are determined to be (50.3±3.1)% and (28.0±1.8)%, respectively. Once the J/ψ is identified, the detection efficiency for $\phi \to K^+K^-$ originating from a $B_s^0 \to J/\psi\phi$ decay is (51.8±5.2)%. The quoted uncertainties for the reconstruction efficiencies are predominantly statistical. Possible sources of systematic errors are from uncertainties in the lepton identification efficiency and B meson fragmentation function. However, these systematic errors are small compared to the overall statistical uncertainties and are ignored.

After correcting for unobserved decay modes and using $B(J/\psi \to \ell^+\ell^-) = (6.27 \pm 0.20)\%$ [20], the overall efficiency for detecting the decay chain $B_s^0 \to e^+e^-K^+K^-$ is (1.21±0.14)%.

From the one observed B_s^0 event, assuming the Standard Model value for $\Gamma_{b\bar{b}}/\Gamma_{had} = 0.217$ [18] and taking into account all errors, we determine:

$$f(\bar{b} \to B_s^0) \cdot B(B_s^0 \to J/\psi\phi) < 0.07\% \quad (90\%\text{C.L.}) \; .$$

3.3 The Decay $B_s^0 \to D_s^-\pi^+$

We search for B_s^0 events in the mode $B_s^0 \to D_s^-\pi^+$, by selecting $D_s^-\pi^+$ combinations with invariant mass between 4.5 and 6.0 GeV/c^2.

D_s^- candidates are identified in the modes $D_s^- \to \phi\pi^-$ and $D_s^- \to K^{*0}K^-$, where ϕ and K^{*0} mesons are reconstructed in the modes $\phi \to K^+K^-$ and $K^{*0} \to K^+\pi^-$. The invariant masses of the ϕ candidates are required to be within ±0.015 GeV/c^2 of the ϕ meson mass and the invariant masses of the K^{*0} candidates within ±0.050 GeV/c^2 of the K^{*0} mass; the latter takes into account the natural width of the K^{*0} resonance [5].

To suppress combinatorial background we exploit specific angular distributions, in a procedure similar to that used to select $B_d^0 \to D^{*-}\pi^+$ decays. We require $|\cos\theta_d| < 0.8$, where θ_d is the angle in the D_s^- rest frame between the direction of the vector meson and the direction of the D_s^- in the laboratory frame. We also require $|\cos\theta_v| > 0.4$, where θ_v is the angle in the rest frame of the vector meson between the direction of the K^+ from the decay of the vector meson and the direction of the D_s^-. Combinations passing the above selection criteria and having an invariant mass within ±0.070 GeV/c^2 of the D_s^- mass are considered D_s^- candidates.

B_s^0 candidates are formed by combining the D_s^- candidates with oppositely charged tracks that are consistent with the pion hypothesis and that are within the same jet. We require $|\cos\theta_b| < 0.8$, where θ_b is the angle in the rest frame of the B_s^0 between the D_s^- direction and the direction of the B_s^0 in the laboratory frame. We also take advantage of the hard fragmentation of the B hadrons and require the momentum of the B_s^0 candidates to exceed 70% of the beam energy.

For each $B_s^0 \to D_s^-\pi^+$ candidate we reconstruct two decay vertices: the decay vertex of the B_s^0 meson and that of the D_s^- decay. We require both decay vertices to be contained in the hemisphere

centred around the B_s^0 momentum vector. Finally we require the B_s^0 decay length (using the average e^+e^- interaction point [21]) divided by the error of the decay length measurement to be greater than one. This requirement, with an efficiency of 75%, is imposed due to the high background level in the $B_s^0 \to D_s^- \pi^+$ mode.

After all selection criteria eight B_s^0 candidates remain in the data sample, with six in the mass range 5.1 to 5.5 GeV/c^2. The measured masses of the B_s^0 candidates with mass above 5.0 GeV/c^2 are shown in Fig. 4, which also includes the $B_s^0 \to J/\psi\phi$ candidate. The error obtained for each candidate is due to the measurement errors of its individual tracks.

In Fig. 5 we show the invariant mass distribution of the $B_s^0 \to D_s^- \pi^+$ candidates, including the $B_s^0 \to J/\psi\phi$ candidate. The hatched histogram corresponds to the $B_s^0 \to D_s^- \pi^+ \to \phi\pi^-\pi^+$ decays, the open histogram to the $B_s^0 \to D_s^- \pi^+ \to K^{*0}K^-\pi^+$ decays and the double hatched histogram to the $B_s^0 \to J/\psi\phi$ decay.

To check the level of the remaining combinatorial background we examine the invariant mass distribution of the wrong-sign combinations, $D_s^- \pi^-$. No such events survive our selection criteria in the mass range studied. We also search for $B_s^0 \to K^+K^-\pi^-\pi^+$ events where the $K^+K^-\pi^-$ combinations do not come from D_s^- decay by selecting side-bands $1.80 < M(K^+K^-\pi^-) < 1.88$ GeV/c^2 and $2.10 < M(K^+K^-\pi^-) < 2.20$ GeV/c^2, on both sides of the D_s^- mass. Three events with $K^+K^-\pi^-\pi^+$ invariant mass below 5.0 GeV/c^2 and one event with invariant mass between 5.1 and 5.5 GeV/c^2 survive our selection criteria. This level of combinatorial background is consistent with that obtained by the fit to Fig. 5, as described below.

Possible sources of $D_s^- \pi^+$ candidates are: (a) the signal, $B_s^0 \to D_s^- \pi^+$; (b) combinatorial background and (c) feed down from higher multiplicity B_s^0 decay modes. Fig. 6 shows the expected signal from Monte Carlo simulation for the decay $B_s^0 \to D_s^- \pi^+$ (solid histogram). The detection efficiencies obtained are (7.4±0.2)% and (5.0±0.3)% in the $D_s^- \to \phi\pi^-$ and $D_s^- \to K^{*0}K^-$ decay modes, respectively. The quoted uncertainties are statistical. The systematic error from modelling of quark fragmentation is found to be less than 1%.

Monte Carlo studies have shown that the decay modes involving the D_s^{*-}, such as $B_s^0 \to D_s^{*-}\pi^+$ with $D_s^{*-} \to D_s^-\gamma$, where the γ is not detected or used in the reconstruction, feed down into the $D_s^-\pi^+$ mass spectrum, and produce a peak about 0.200 GeV/c^2 below the B_s^0 mass (Fig. 6, dashed histogram). Another feed-down effect is due to the possible decay $B_s^0 \to D_s^- \rho^+$, which gives a broad structure near the B_s^0 mass (Fig. 6, dotted histogram). In Fig. 6 the normalisations of these contributions are made according to the relative detection efficiencies. Since the separation between the true and the feed-down peaks is comparable to the mass resolution, the overall mass distribution will show one broad enhancement. Monte Carlo studies also show that the background from B_d^0 decays with similar topology, where a pion is mis-identified as a kaon, is negligible.

The invariant mass distribution of Fig. 5 was fitted to a linear combination of functions representing the various sources of $B_s^0 \to D_s^- \pi^+$ and $B_s^0 \to J/\psi\phi$ candidates: a Gaussian with a width of 0.075 GeV/c^2 representing the $B_s^0 \to D_s^- \pi^+$ decays (dashed curve); a Gaussian with a width of 0.120 GeV/c^2 centred 0.200 GeV/c^2 below the central value of the first Gaussian, representing the $B_s^0 \to D_s^{*-}\pi^+$ decays (dotted curve); and a combinatorial background term whose shape is determined from background events in the same kinematical region (dashed-dotted curve). The expected contribution of $B_s^0 \to D_s^- \rho^+$ decays is sufficiently small that no extra term need be used in the fit. For the $B_s^0 \to D_s^- \pi^+$ decay the fit obtains 5.4 ± 2.6 events at a mass of 5.370 ± 0.040 GeV/c^2. This is consistent with the mass measurement from the $B_s^0 \to J/\psi\phi$ event. For the $B_s^0 \to D_s^{*-}\pi^+$ and $B_s^0 \to J/\psi\phi$ decays the fit obtains 0.9 ± 1.6 events. The background level obtained is 0.7 ± 0.5 events between 5.1 and 5.5 GeV/c^2. In

addition, we repeated the analysis using different sets of cuts. The observed numbers of candidates were within expectations.

To calculate an upper limit on the decay rate for $B_s^0 \to D_s^- \pi^+$ we conservatively assume that the six $D_s^- \pi^+$ entries in Fig. 5 between 5.1 and 5.5 GeV/c^2 all originate from the B_s^0, with no background. Assuming the Standard Model value for $\Gamma_{b\bar{b}}/\Gamma_{had} = 0.217$ [18], we obtain

$$f(\bar{b} \to B_s^0) \cdot B(B_s^0 \to D_s^- \pi^+) < 1.3\% \quad (90\% \text{ C.L.}) ,$$

where we have used the ratio $B(D_s^- \to K^{*0}K^-)/B(D_s^- \to \phi\pi^-)$ from refer. [5] to average over the two decay modes of the D_s^-.

4 Summary and Conclusion

In 1.23×10^6 hadronic Z^0 decays recorded with the OPAL detector at LEP, we have searched for B mesons in three different decay modes. We have measured the $B_d^0 \to D^{*-}\pi^+$ branching ratio and production branching ratios for the $B_s^0 \to J/\psi\phi$ and $B_s^0 \to D_s^-\pi^+$ decays assuming the Standard Model value for $\Gamma_{b\bar{b}}/\Gamma_{had} = 0.217$ [18]. From 8.1 ± 2.9 reconstructed $B_d^0 \to D^{*-}\pi^+$ events, we obtain the branching ratio for this mode to be

$$B(B_d^0 \to D^{*-}\pi^+) = 1.0 \pm 0.4(\text{stat.}) \pm 0.1(\text{syst.})\% ,$$

using a B_d^0 production fraction $f(\bar{b} \to B_d^0) = 0.38$. From one reconstructed event in the mode $B_s^0 \to J/\psi\phi$ we determine the B_s^0 mass to be

$$M_{B_s^0} = 5.359 \pm 0.019 \pm 0.007 \text{ GeV}/c^2$$

and obtain

$$f(\bar{b} \to B_s^0) \cdot B(B_s^0 \to J/\psi\phi) < 0.07\% \quad (90\% \text{ C.L.}) .$$

A cluster of six events is found near this mass in the mode $B_s^0 \to D_s^-\pi^+$. From a fit to the invariant mass distribution of these events we find a mass of 5.370 ± 0.040 GeV/c^2, consistent with that obtained from the single $B_s^0 \to J/\psi\phi$ event. We obtain

$$f(\bar{b} \to B_s^0) \cdot B(B_s^0 \to D_s^-\pi^+) < 1.3\% \quad (90\% \text{ C.L.}) .$$

5 Acknowledgements

It is a pleasure to thank the SL Division for the efficient operation of the LEP accelerator, the precise information on the absolute energy, and their continuing close cooperation with our experimental group. In addition to the support staff at our own institutions we are pleased to acknowledge the
Department of Energy, USA,
National Science Foundation, USA,
Texas National Research Laboratory Commission, USA,
Science and Engineering Research Council, UK,
Natural Sciences and Engineering Research Council, Canada,
Fussefeld Foundation,
Israeli Ministry of Energy and Ministry of Science,

Minerva Gesellschaft,
Japanese Ministry of Education, Science and Culture (the Monbusho) and a grant under the Monbusho International Science Research Program,
German Israeli Bi-national Science Foundation (GIF),
Direction des Sciences de la Matière du Commissariat à l'Energie Atomique, France,
Bundesministerium für Forschung und Technologie, Germany,
National Research Council of Canada,
A.P. Sloan Foundation and Junta Nacional de Investigação Científica e Tecnológica, Portugal.

References

[1] CLEO Collab., D. Bortoletto et al., Phys. Rev. **D 45** (1992) 21;
ARGUS Collab., H. Albrecht et al., Z. Phys. **C 48** (1990) 543.

[2] ALEPH Collab., D. Buskulic et al., Phys. Lett. **B 322** (1994) 275;
Phys. Lett. **B 297** (1992) 449; Phys. Lett. **B 294** (1992) 145; Phys. Lett. **B 278** (1992) 209;
DELPHI Collab., P. Abreu et al., Z. Phys. **C 61** (1994) 407;
Phys. Lett. **B 311** (1993) 379; Phys. Lett. **B 289** (1992) 199;
OPAL Collab., R. Akers et al., Phys. Lett. **B 316** (1993) 435; P.D. Acton et al., Phys. Lett. **B 312** (1993) 501; Phys. Lett. **B 295** (1992) 357; Phys. Lett. **B 281** (1992) 394.

[3] OPAL Collab., P.D. Acton et al., Phys. Lett. **B 295** (1992) 357.

[4] ALEPH Collab., D. Buskulic et al., Phys. Lett. **B 311** (1993) 425; Phys. Lett. **B 316** (1993) 631;
CDF Collab., F. Abe et al., Phys. Rev. Lett. **71** (1993) 1685;
DELPHI Collab., P. Abreu et al., CERN-PPE/94-22, Submitted to Phys. Lett. **B**.

[5] Review of Particle Properties, Phys. Rev. **D 45** (1992) 1.

[6] J. Bijnens and F. Hoogeveen, Phys. Let. **B 283** (1992) 434.

[7] OPAL Collab., K. Ahmet, et al., Nucl. Inst. and Meth. **A 305** (1991) 275.

[8] P.P. Allport et al., Nucl. Inst. and Meth. **A 324** (1993) 34.

[9] O. Biebel et al., Nucl. Inst. and Meth. **A 323** (1992) 169.

[10] M. Hauschild et al., Nucl. Inst. and Meth. **A 314** (1992) 74.

[11] OPAL Collab., G. Alexander et al., Z. Phys. **C 52** (1991) 175.

[12] OPAL Collab., P.D. Acton et al., Z. Phys. **C 58** (1993) 523.

[13] T. Sjöstrand, Int. J. of Mod. Phys. **A 3** (1988) 751.

[14] J. Allison et al., Nucl. Instrum. and Meth. **A 317** (1992) 47.

[15] C. Peterson et al., Phys. Rev. **D 27** (1983) 105.

[16] OPAL Collab., R. Akers et al., Z. Phys. **C 60** (1993) 199.

[17] JADE Collab., S. Bethke et al., Phys. Lett. **B 213** (1988) 235.

[18] D. Bardin et al., CERN-TH.6443/92 (1992) (unpublished).

[19] The relative yield of various b-flavoured hadrons is a function of the production rates of $u\bar{u}$, $d\bar{d}$ and $s\bar{s}$ pairs, and diquarks in the fragmentation process. Monte Carlo models which have been tuned to the data on strange and charmed hadron production in e^+e^- annihilations suggest a B_d^0 production fraction $f(\bar{b} \to B_d^0) = 0.38$. For reviews see:
T. Sjøstrand et al., in Z^0 Physics at LEP I, ed. G. Altarelli, et al., CERN 89-08, Vol 3 (1989) 143;
D.H. Saxon, "Quark and Gluon Fragmentation", in High Energy Electron Positron Annihilations, ed. A. Ali and P. Söding, pub. World Scientific;
D. Bortoletto et al., Phys. Rev. **D 37** (1988) 1719.

[20] S.Y. Hsueh and S. Palestini, Phys. Rev. **D 45** (1992) 2181.

[21] OPAL Collab., P.D. Acton et al., Z. Phys. **C 60** (1993) 217.

Figure Captions

Fig. 1. Invariant mass distribution of $D^{*-}\pi^+$ candidates in data. The solid curve is a fit with Gaussians representing the $B_d^0 \to D^{*-}\pi^+$ and $B_d^0 \to D^{*-}\rho^+$ decays, plus a flat distribution for the combinatorial background.

Fig. 2. Invariant mass distribution of $D^{*-}\pi^+$ candidates from Monte Carlo simulated B_d^0 decays in the modes $B_d^0 \to D^{*-}\pi^+$ (solid) and $B_d^0 \to D^{*-}\rho^+$ (dashed). The normalisations of these contributions are made according to the relative branching ratios.

Fig. 3. Display of the $B_s^0 \to J/\psi\phi$ event in the plane perpendicular to beam direction showing the e^+e^- from the J/ψ decay and the K^+K^- from the ϕ decay in the central tracking chambers. The dark shaded rectangles correspond to the measured energy deposited in the electromagnetic calorimeter.

Fig. 4. Invariant mass measurements of the seven B_s^0 candidates. The errors on the invariant masses are obtained from the errors and covariances of the measured track parameters.

Fig. 5. Invariant mass distribution of the $D_s^-\pi^+$ and $J/\psi\phi$ candidates. The hatched histogram corresponds to the $B_s^0 \to D_s^-\pi^+ \to \phi\pi^-\pi^+$ decays, the open histogram to the $B_s^0 \to D_s^-\pi^+ \to K^{*0}K^-\pi^+$ decays and the double hatched histogram to the $B_s^0 \to J/\psi\phi$ decay. The curves represent a fit with a a Gaussian for the $B_s^0 \to D_s^-\pi^+$ decay (dashed), a Gaussian for the $B_s^0 \to D_s^{*-}\pi^+$ decay (dotted) and a parametrisation for the background (dashed-dotted).

Fig. 6. Invariant mass distribution of the $D_s^-\pi^+$ combinations from simulated B_s^0 decays in the modes $B_s^0 \to D_s^-\pi^+$ (solid), $B_s^0 \to D_s^{*-}\pi^+$ (dashed) and $B_s^0 \to D_s^-\rho^+$ (dotted). The normalisations of these contributions are made according to the relative detection efficiencies.

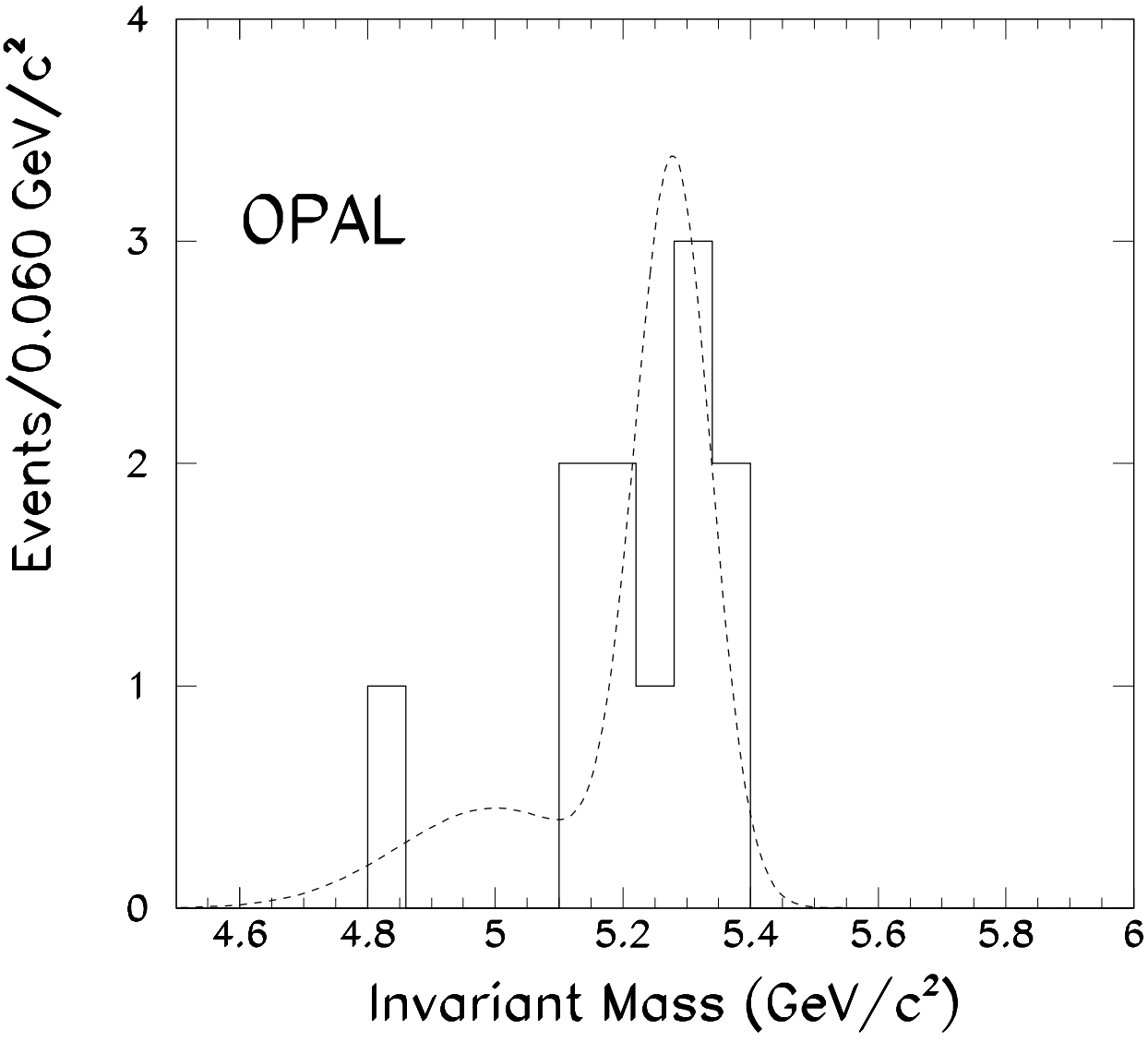
OPAL
Events/0.060 GeV/c²
Invariant Mass (GeV/c²)
0
1
2
3
4
4.6
4.8
5
5.2
5.4
5.6
5.8
6

Fig. 1

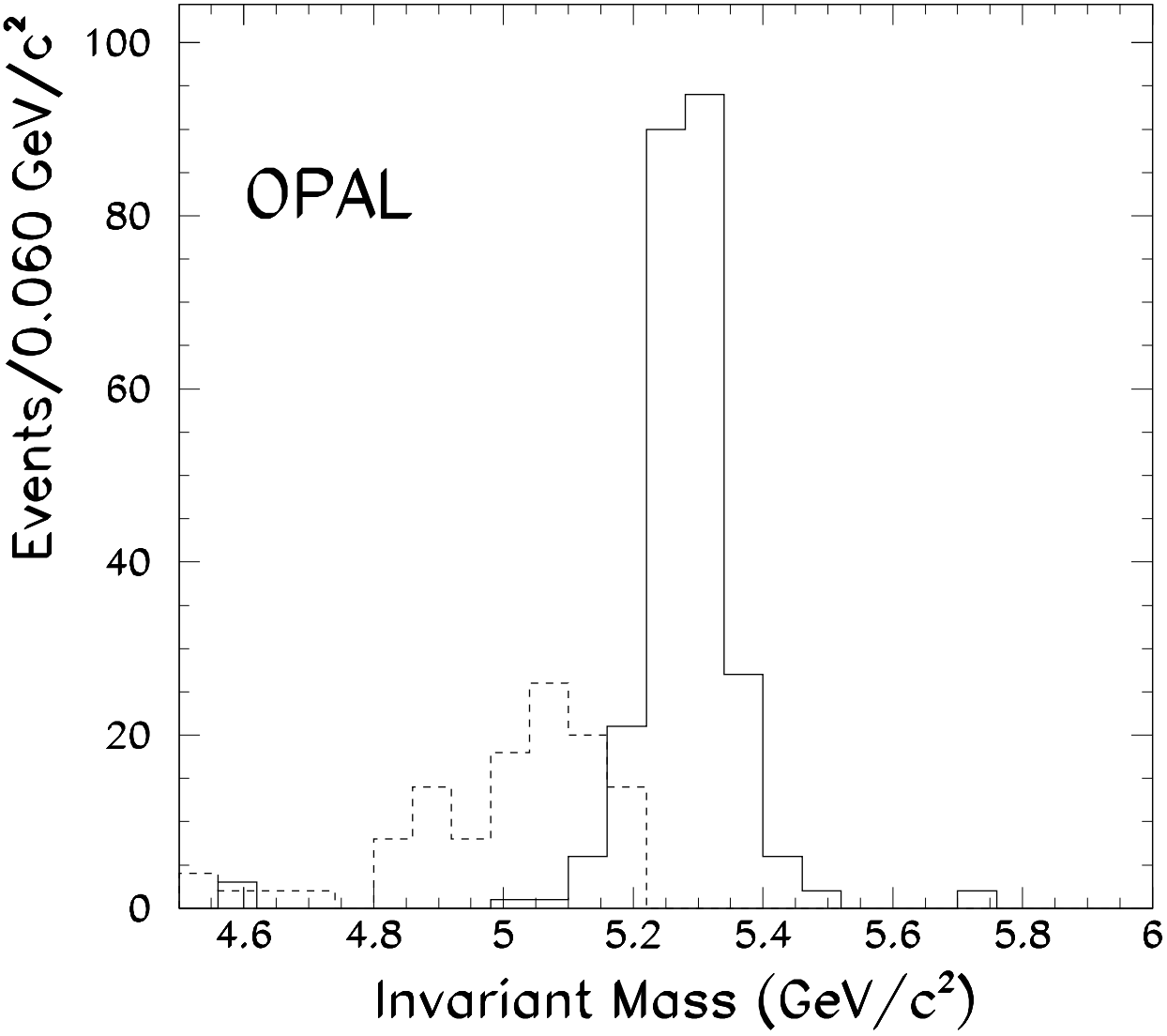
OPAL
Events/0.060 GeV/c²
100
80
60
40
20
0
4.6
4.8
5
5.2
5.4
5.6
5.8
6
Invariant Mass (GeV/c²)

Fig. 2

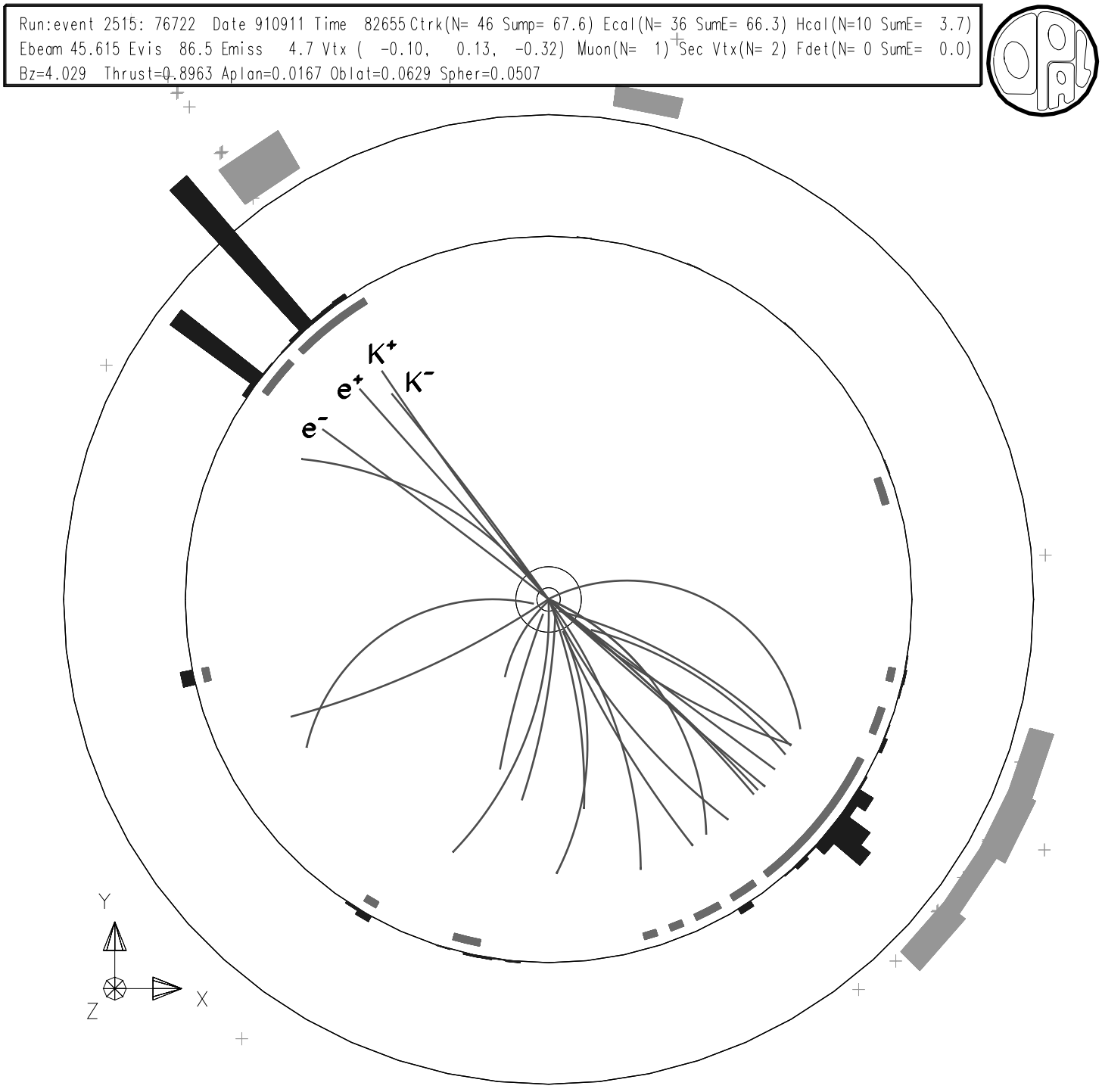
Run:event 2515: 76722 Date 910911 Time 82655 Ctrk(N= 46 Sump= 67.6) Ecal(N= 36 SumE= 66.3) Hcal(N=10 SumE= 3.7)
Ebeam 45.615 Evis 86.5 Emiss 4.7 Vtx (-0.10, 0.13, -0.32) Muon(N= 1) Sec Vtx(N= 2) Fdet(N= 0 SumE= 0.0)
Bz=4.029 Thrust=0.8963 Aplan=0.0167 Oblat=0.0629 Spher=0.0507
K+
e+
K-
e-
Y
Z
X

Fig. 3

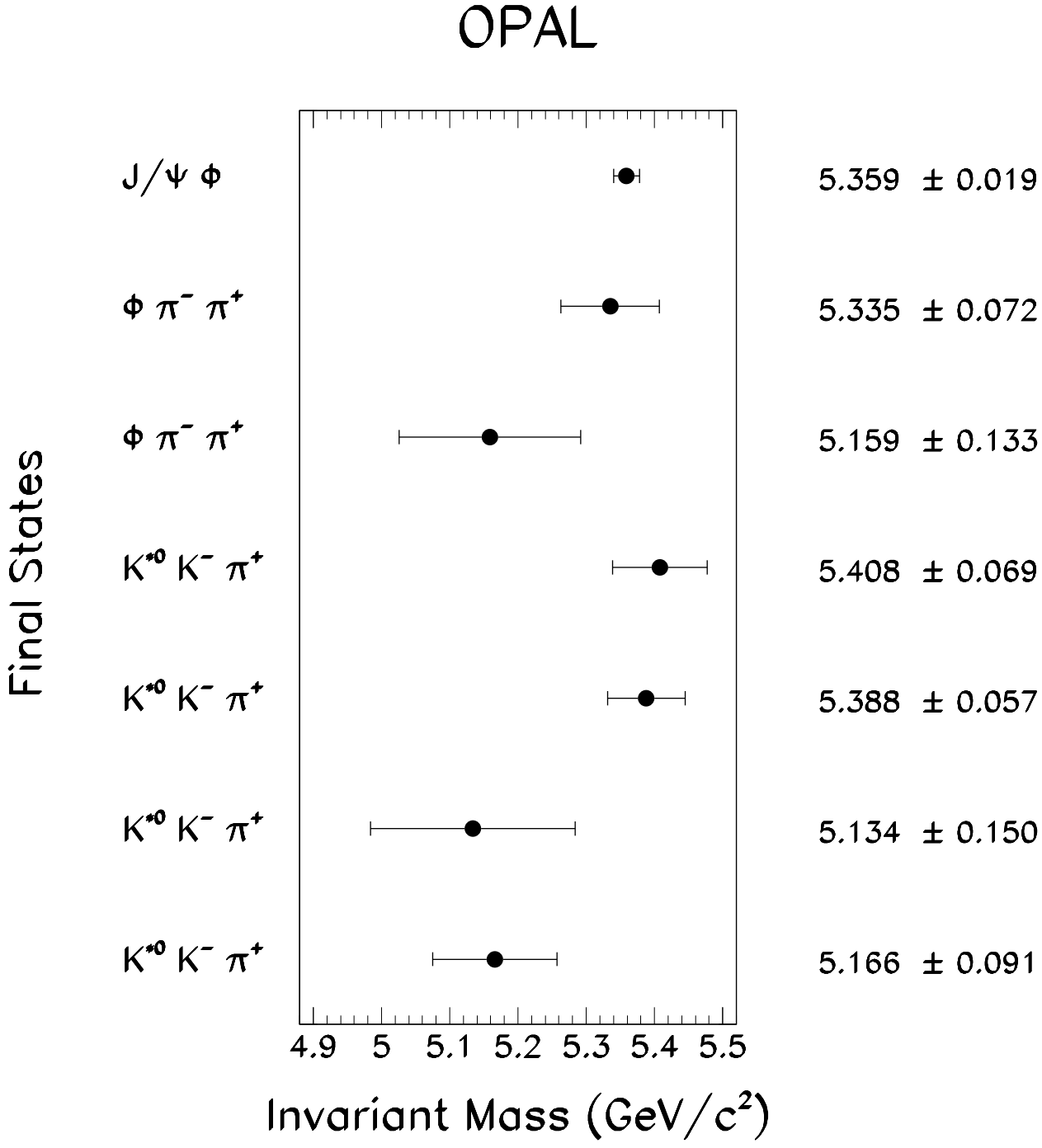
OPAL
J/ψ φ
φ π⁻ π⁺
φ π⁻ π⁺
K*0 K⁻ π⁺
K*0 K⁻ π⁺
K*0 K⁻ π⁺
K*0 K⁻ π⁺
5.359 ± 0.019
5.335 ± 0.072
5.159 ± 0.133
5.408 ± 0.069
5.388 ± 0.057
5.134 ± 0.150
5.166 ± 0.091
Final States
4.9
5
5.1
5.2
5.3
5.4
5.5
Invariant Mass (GeV/c²)

Fig. 4

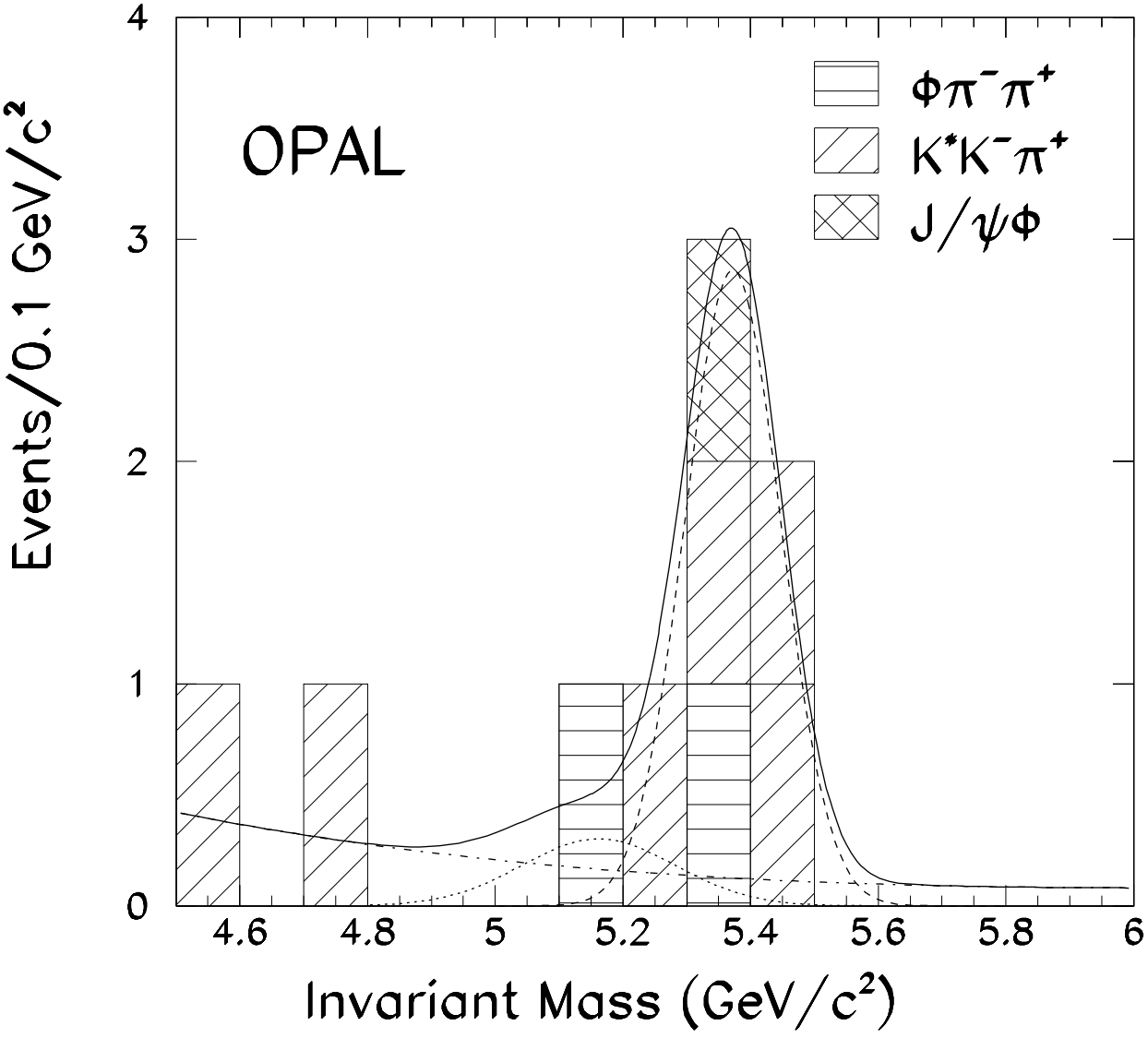
OPAL
$\Phi\pi^-\pi^+$
$K^*K^-\pi^+$
$J/\psi\Phi$
Events/0.1 GeV/c^2
Invariant Mass (GeV/c^2)
0
1
2
3
4
4.6
4.8
5
5.2
5.4
5.6
5.8
6

Fig. 5

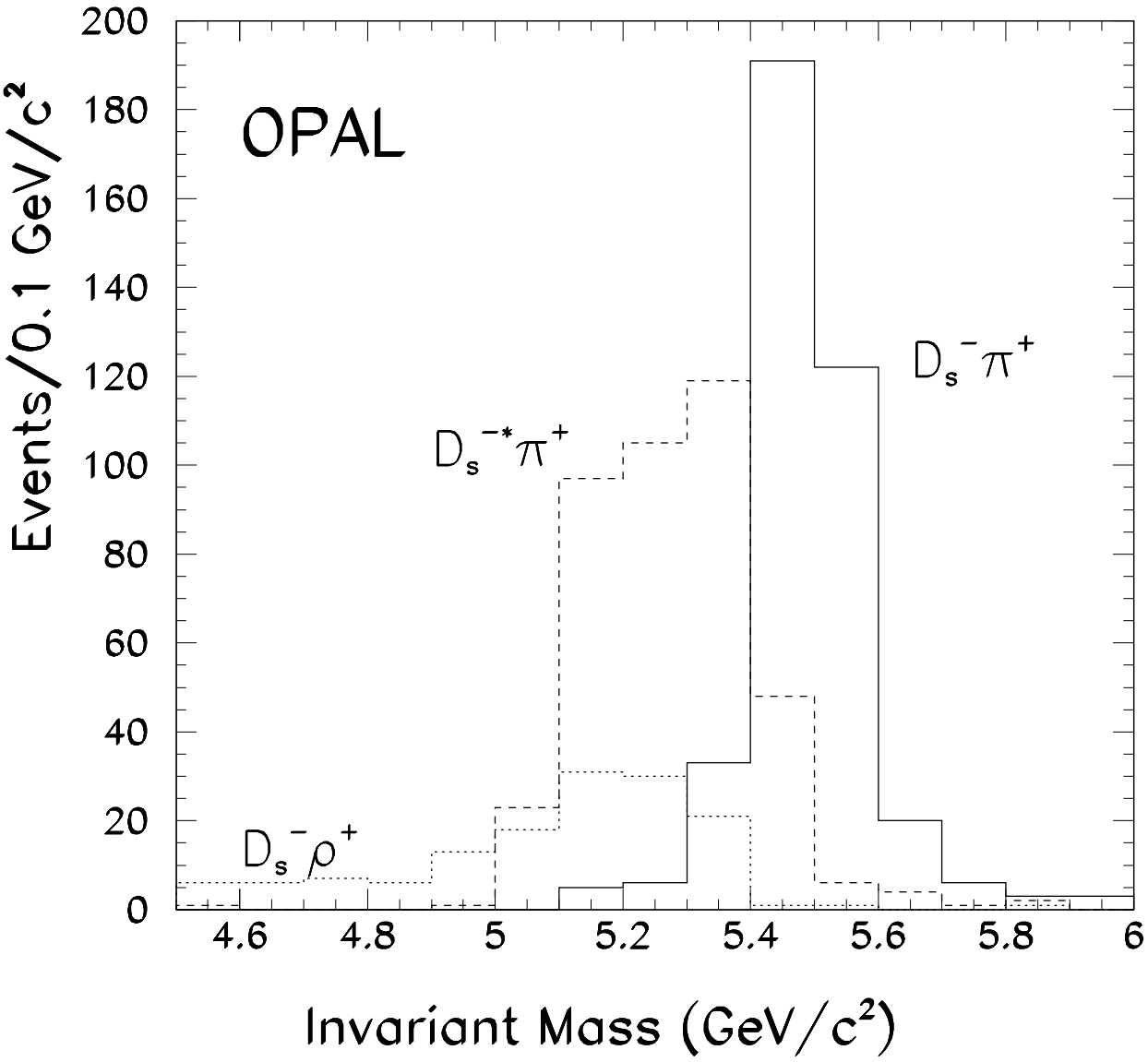
OPAL
Events/0.1 GeV/c²
Invariant Mass (GeV/c²)
$D_s^- \pi^+$
$D_s^{-*} \pi^+$
$D_s^- \rho^+$
0
20
40
60
80
100
120
140
160
180
200
4.6
4.8
5
5.2
5.4
5.6
5.8
6

Fig. 6